

Biosynthesis, characterization and remedial aspect of silver nanoparticles against pathogenic bacteria

Abstract

Silver nanoparticles are multifunctional nanoparticles with effective antibacterial activity. In this present study, the synthesized AgNPs by reduction of silver nitrate during exposure to betel leaf aqueous extract was confirmed by UV-Vis spectrum, the SPR peak observed at 443nm. The characterization of AgNPs was carried out using Fourier transform infrared spectroscopy, X-ray diffraction, Dynamic Light Scattering, Scanning Electron Microscope and Energy-Dispersive Spectroscopy. XRD analysis revealed that the particles were crystalline in nature with face-centered cubic geometry. The distribution of the AgNPs observed that the particles obtained are polydisperse mixtures in the size range from 70 to 80nm by using DLS analysis. SEM image of AgNPs shown that relatively spherical in shape and uniform with high agglomeration were noted. AgNPs coated IVC have shown the greatest antibacterial activity against biofilm producing human pathogens such as *E. coli*, *S. aureus*, *P. aeruginosa*, *S. epidermidis* and *K. pneumoniae*.

Keywords: silver nanoparticles, betel leaf, antibiofilm activity, intravascular catheter, pathogens

Volume 4 Issue 3 - 2018

Ranjith Kumar Rajamani,¹ Selvam Kuppusamy,² Chandar Shekar Bellan,³ Pratheep Hallan Ravi,⁴ P Sagadevan⁵

¹Department of Biotechnology, Nehru Arts and Science College, India

²Department of Botany, Periyar University, Salem, India

³Nanotechnology Research Lab, Department of Physics, Kongunadu Arts and Science College, India

⁴Department of Physics, Government Arts College, India

⁵Department of Biotechnology, KG College of Arts and Science, India

Correspondence: Ranjith kumar Rajamani, Department of Biotechnology, Nehru Arts and Science College, Coimbatore, Tamilnadu -641105, Tamilnadu, India,
Email biotechranjith@gmail.com

Received: January 21, 2018 | **Published:** May 02, 2018

Abbreviations: IVC, intravascular catheters; FTIR, fourier transform infrared spectrometer; DLS, dynamic light scattering

Introduction

Bacterial biofilms are widely distributed and play important roles in many environments. Generally, biofilms are bacterial communities in which cells are embedded in a matrix of extracellular polymeric compounds attached to a surface.¹ Bacterial surface components and extracellular compounds in combination with environmental and quorum-sensing signals are crucial for autoaggregation and biofilm development in most bacterial species.^{2,3} Rinaudi & Giordano⁴ suggested the basic accepted model of biofilm formation, environmental signals trigger the process and flagella are required for the biofilm community to approach and move across the surface. The initial steps of attachment are mediated by outer membrane proteins, pili or lipopolysaccharides. After the formation of microcolonies, the production of quorum-sensing signals is required for the formation of a mature biofilm. Exopolysaccharides provide the architectural form of biofilms and stabilize their 3-dimensional structure.⁴ The bacteria gain numerous advantages from living in biofilms, including protection from predation, desiccation and exposure to antibacterial substances.⁵ Biofilms contain great implication for public health, since biofilm associated microorganisms exhibit dramatically decreased susceptibility to antimicrobial agents. This may be as a natural outcome of growth or due to transfer extrachromosomal elements to susceptible organisms in the biofilm.⁶

Many urinary tract infections and bloodstream infection are associated with indwelling medical devices and biofilm associated. The most strategy for treating these infections may be deletion and removal of the biofilm contaminated device. Urinary tract infections and bloodstream infection are associated with indwelling medical devices and biofilm associated. The most strategy for treating these

infections may be deletion and removal of the biofilm contaminated device. Urinary catheter biofilms may initially be composed of single species, but longer exposures inevitably lead to multispecies biofilms.⁷ Intravascular catheters (IVC) are used for the administration of medications, parenteral nutrition, fluids and blood products to monitor hemodynamic status and to provide hemodialysis.⁸ Use of IVC for patient care may be associated with increased risk of central line associated bloodstream infection. Mermel (2000) study reported around 80,000 central line associated bloodstream infection occur among patients in US intensive care units each year.⁹ Anaissie and co-worker reported that the biofilms may form within three days after catheter insertion.¹⁰

Nanotechnology is novel approaches to research phenomena at atomic, molecular and macromolecular scales, where properties differ significantly from those at a larger scale.¹¹ Nanomaterials have nanoscale dimensions about between 1-100nm and frequently exhibit new and significantly chemical, physical and biological changed proprieties¹² and nanoparticles have excellent catalysts, sensor and adsorbents due to their large specific surface area and high reactivity.¹³ Several engineered and natural nanoparticles including titanium dioxide,¹⁴ zinc,¹⁵ silver¹⁶ and gold¹⁷ have shown strong antimicrobial properties against human pathogens. Nanobiotechnology has arisen due to assimilation of biotechnology with nanotechnology for emerging biosynthetic and eco-friendly approach for synthesis of nanoparticles.¹⁸ The novel method for synthesizing nanoparticles utilizing biological resource and such a methodology is called as “green chemistry”.¹⁹ Shanmugavadi and co-workers revealed that green synthesis approaches of producing silver nanoparticles using pomegranate peel extract have benefits over the conventional techniques and they own potential antibacterial activity against human pathogens.²⁰ Antimicrobial activities of nanoparticles are well-known, particularly, silver nanoparticles have been described as the one with the highest level of toxicity for microorganisms and lowest toxicity

for animal cells.²¹ Research studies on the biological synthesis silver nanoparticles have recently appeared as new antimicrobial agents due to their high surface area to volume ration and unique chemical and physical properties.²²⁻²⁴ In addition the improvement of impregnation of medical devices with silver nanoparticles is that it protects both outer and inner surfaces of medical devices and there is continuous release of silver ions providing good antimicrobial activity.^{25,26} Ansari and co-workers study demonstrated the anti-biofilm efficacy of silver nanoparticles against methicillin resistance *S. aureus* and methicillin resistance *S. epidermidis* isolated from wounds.²⁷ Hence, the present study was designed to enhance our knowledge of betel leaf mediated green synthesized silver nanoparticles impregnated intravascular catheters tried against biofilm producing bacteria such as *Escherichia coli*, *Staphylococcus aureus*, *Pseudomonas aeruginosa*, *Staphylococcus epidermidis* and *Klebsiella pneumoniae*.

Materials methods

Materials

The chemical silver nitrate (AgNO_3) was purchased from SD Fine Chemical Pvt Ltd, Mumbai.

Preparations of the betel leaf extract

Apparently healthy betel leaves were collected from local market and washed thoroughly in tap water to remove dirt and other attached particles. The betel leaves extract was prepared by taking 20g of thoroughly washed and finely cut betel leaf in a 250ml Erlenmeyer flask with 100ml of sterile distilled water and then boiled the mixture for 10min. The solution was then removed from the heat source and left at room temperature. Following this step the extract was then filtered through a Whatman filter paper No.1. The extract was kept in refrigerator at 4 °C for further experiments.

Biosynthesis of AgNPs from betel leaf

The aqueous solution of 1mM concentration silver nitrate (AgNO_3) was prepared to synthesize silver nanoparticles from betel leaves. For the experiment briefly, 5ml of betel leaves aqueous extract was slowly added to 100ml of aqueous solution of 1mM concentration AgNO_3 while stirring, for reduction into Ag ions. The formation of dark brown colour was observed after 8h incubation at room temperature and λ max was taken using UV-Visible spectroscopy (UV-2600 series shimadzu UV-vis spectrophotometer from 200-800nm at a resolution of 1nm). Then the silver nanoparticles solution was purified by repeated centrifugation at 10,000 rpm for 20min to isolate Ag nanoparticles free from other bioorganic compounds present in the solution. After centrifugation the obtained particles were washed with distilled water for 2 to 3min and kept it in Hot air oven for drying at 60°C for 2hours. The effectiveness and accuracy in results without any contamination, each and every steps of the experiment were maintained under sterility conditions.

Characterization of AgNPs

Several analytical techniques are available for the structural, compositional analysis of the nanoparticles. The betel leaves aqueous extract mediated bioinspired synthesized silver nanoparticles were characterized by Fourier Transform Infrared Spectrometer (FTIR) analysis obtained in the range from 4,000 to 400cm⁻¹ on Tracer-100 shimadzu FT-IR spectrophotometer. The structural characterization of the silver nanoparticles obtains by using X-ray diffractometer

(SHIMADZU Lab X XRD-6000 serious) with a $\text{CuK}\alpha$ radiation monochromatic filter in the range 10-80°. Debye-Scherrer's equation was used to determine the particle size of the silver nanoparticles from the 2 θ values of the X-ray diffraction peaks. Debye-Scherrer's equation $D=k\lambda/\beta\cos\theta$, Where, k - constant, λ -wavelength of the X-ray, β -full width half maximum of the XRD peak (radians), θ -Bragg's angle of the XRD peak. The particles size were arrived based on measuring the time dependent fluctuation of scattering of laser light by the nanoparticles using Dynamic Light Scattering (DLS). The obtained data were analyzed using zetasizer software. The morphological characterizations of the bioinspired synthesized silver nanoparticle samples were done using Scanning Electron Microscope (SEM) JEOL model 6390 and Energy-Dispersive Spectroscopy (EDS) used for the elemental analysis or chemical characterization of a sample were performed on Hitachi S-3400 NSEM instrument equipped with a Thermo EDS attachments.

Assessing the biofilm forming capability of test bacteria

The efficiency of test organisms to form biofilm capability was determined using Microtitre plate (MTP) biofilm assay.²⁸ Briefly, in this method bacterial attachment to an abiotic surface is assessed by measuring the stain taken up by adherent biomass in a 96-well plate format by means of MTP assay. The test organisms such as *E. coli*, *S. aureus*, *P. aeruginosa*, *S. epidermidis* and *K. pneumoniae* were grown in 96-well Microtitre plate for 48 h. The cells remaining adhered to the wells were subsequently stained with a dye that allowed visualization of the attachment pattern. Both of all test organisms was inoculated in a 5ml culture broth and grown to stationary phase and cultures were diluted at 1:100. Subsequent, 100 μ l of each diluted cultures was pipetted into eight wells in a fresh Microtitre plate. The plate was covered and incubated at optimal growth temperature for 24-48h. Four small trays were set up in a series and 1 to 2inches of tap water was added to the last three. The first tray was used to collect waste, while the others were used to wash the assay plates. Unbound bacteria if any were removed from each Microtitre dish by briskly shaking the dish out over the waste tray. In addition, 125 μ l of 0.1% crystal violet solution was added to each well and staining was done for 10min at room temperature. The crystal violet solution was removed by shaking each Microtitre dish out over the waste tray. The dishes were washed successively in each of the next two water trays and as much liquid as possible was shaken out after each wash. To remove any excess liquid, each Microtitre dish was inverted and vigorously tapped on paper towels. The plates were allowed to air-dry and added 200 μ l of 95% ethanol to each stained well. The plates were covered to allow solubilisation by incubating for 10 to 15min at room temperature and the substances of each well were concisely mixed by pipetting. Subsequent 125 μ l of the crystal violet-ethanol solution was transferred from each well to a separate well in an optically clear flat-bottom 96-well plate. The optical density (OD) of each of these 125 μ l samples was measured at a wavelength of 550 to 580nm. Optical density (OD) of stained adherent bacteria was determined with a micro ELISA auto reader. The optical density values were considered as an index of bacteria adhering to surface and forming biofilms.

Preparation of AgNPs coated IVC

AgNPs releasing intravascular catheters were made using slurry-dipping technique. The technique started with the preparation of stable slurry with 0.5g of bioinspired AgNPs in the molten

Polyethylene glycol (PEG) and appropriate slurry temperature (37°C) was determined by an optimization process based on a trial-and-error approach to achieve optimum coating thickness, uniformity and stability of composite coating as well as adequate infiltration of AgNPs particles into coating structure. 2g of PEG with a predefined molecular weight was mixed with AgNPs (0.5g) in a glass vial. The mixture was heated at the range of 60-70°C in a water bath to obtain homogeneous slurry. The resulting slurry was homogenized in a magnetic stirrer for 5 to 10min. Each piece of catheter (length 6mm) was dip-coated twice with intermittent drying (suspension coating method). The dip-coating procedure was carried out in sterile glass beakers on a shaker at 120rpm for 30min, with a drying period of about 15min between the two coating procedures, followed by drying at room temperature. All coating steps were carried out under strict aseptic conditions. All samples were coated by a thickness of about 3-10% of catheters outer diameters and the catheter samples were stored at 4°C for up to 15min. In order to increase AgNPs loading and prevent excessive increase in catheter thickness, the coating process was repeated four times for each sample. Subsequently, in order to slow down the release rate of AgNPs from PEG coating and mitigate the friction effect between catheter surface and mucosa, second coating layer was formed on the catheter surface. PVA was dissolved in DMSO to acquire a 10w/w% solution. PEG-coated samples were submerged into PVA solution three times for 1min each. Thereafter, these samples were stored at 4°C or in a deep freezer to implement one freeze-thaw cycle and physically crosslink the samples. The coated intravascular catheters were left to dry on a clean bench for one week at room temperature to remove residual DMSO.

Antibacterial activity of AgNPs coated IVC

The antibacterial activity of catheter materials after dip-coating with AgNPs was performed against biofilm producing bacteria. In this qualitative method the pre-measured size length 6mm of catheter materials were placed on the surface of Mueller-Hinton agar plate which had previously been seeded with an overnight broth culture of the test organisms. The plates were incubated at 37°C for 24 to 48h. The experiment was carried out in triplicate. Antibacterial activity was expressed as the diameter of the zone of inhibition.

Persistence test

Serial plate transfer test (SPTT) was performed to determine the persistence of AgNPs content in the biomaterial during the implantation period. The test was performed after the qualitative antibacterial activity. Briefly, using a sterile swab the overnight broth culture of the test organisms were swabbed on sterile Mueller-Hinton agar (MHA) plates. Each biomaterial coated with bioinspired AgNPs was placed on the seeded MHA plate and incubated at 37°C for 24h. The zone of inhibition was measured and the AgNPs coated biomaterial was immediately transferred to the next MHA plate seeded with similar test bacteria. It was ensured that the same material surface was in contact with the MHA surface. The process was continued until no more inhibitory zone was observed for the biomaterial.

Results and discussion

Biodiversity of plants and their potential secondary constituents, plants and plant parts have gained attention in recent years as medium for nanoparticles synthesis.²⁹ In the present study, the aqueous extract of betel leaf was used as reducing agent for the synthesis of AgNPs using 1mM concentration of AgNO₃. The crude aqueous extract was

light brown colour however after addition of AgNO₃ the colour of the reaction mixture turned dark brown colour which indicated the formation of AgNPs after 6 h incubation period (Figure 1). Green synthesis silver nanoparticles using aqueous seed extract of *J. curcas* and no toxic chemicals are used as reducing and stabilizing agent during the synthesis.³⁰ The synthesized AgNPs by reduction of silver nitrate during exposure to betel leaves aqueous extract was confirmed by UV-Vis spectral analysis, the surface plasmon resonance peak observed at 443nm (Figure 2). Previously researcher reported piper betel leaf petiole extract and ionic surfactants such as cetyltrimethylammonium bromide and sodium dodecyl sulphate were used to prepare the stable AgNPs and the obtained AgNPs are in the size of 80nm.³¹

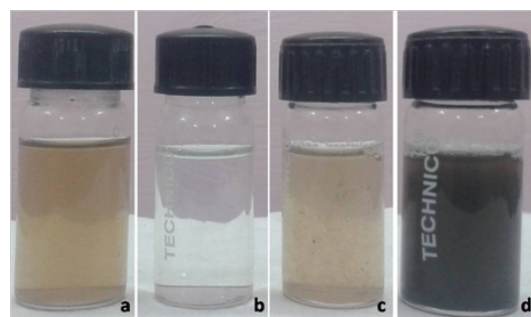


Figure 1 Colour change of betel leaf extracts containing AgNPs before and after synthesis (A) Betel leaf extracts (B) 1mM AgNO₃ (C) before synthesis and (D) after 6h incubation.

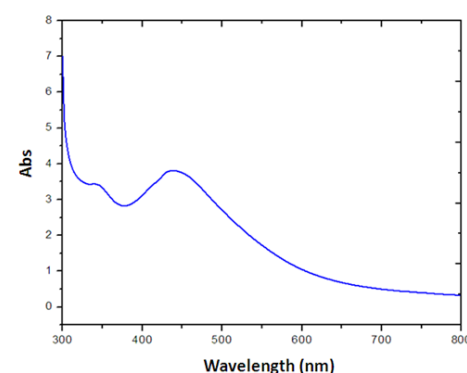


Figure 2 UV absorption spectrum of AgNPs.

Characterization of AgNPs

FTIR spectrum analysis of the reaction mixture has helped to understand the nature of biomolecules involved in the formation of silver nanoparticles.¹¹ The FTIR Spectrogram (Figure 3) of the betel leaf extract mediated bioinspired synthesized AgNPs has showed prominent sharp absorption peaks located 3371.57, 1635.64, 1365.60 and 1219.01. The light peaks located 3788.19, 2808.36, 2646.34, 2183.42 and 2152.56. The absorption peak at 3371.57 cm⁻¹ may be assigned to the O-H stretch, function group of alcohols, phenols and peak at 1635.64 cm⁻¹ is assigned to C=O stretch function of amide compound. Followed by absorption peak at 1365.60 and 1219.01 cm⁻¹ were assigned to S=O stretch and C-N stretch, functional group of sulfones, sulfonyl and amines respectively. The light absorption peaks at 2808.36 and 2646.34 were assigned as C-H stretch functional groups of alkenes and aldehydes. The peak at 2183.42 and 2152.56 cm⁻¹ were

close to C≡C and C=C stretch functional groups of alkynes. Since, the FTIR spectra analysis indicates various functional groups present at different position. *Millingtonia hortensis* mediated biological synthesis silver nanoparticles showed strong and light absorption bands and indicated presence of functional biomolecules such as alcohols, ethers, carboxylic acid ester, alkyl halide.³² Biological components are known to interact with metal salts via these functional groups and mediate their reduction to nanoparticles.³⁰ Hence, the existence of these functional groups is responsible for the stabilization of synthesized silver nanoparticles and also acts as reducing and capping agent.²³

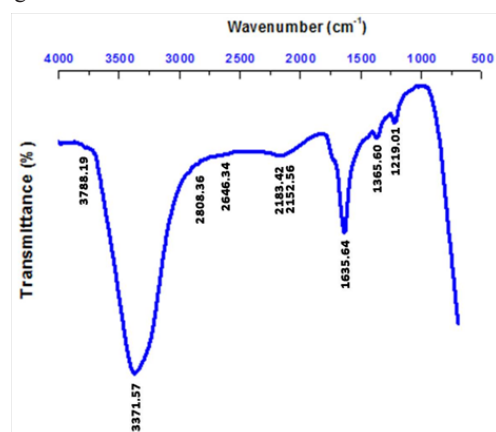


Figure 3 FTIR spectrum of AgNPs.

Analysis through X-ray diffraction was carried out to confirm the crystalline nature of the silver nanoparticles.^{24,33} The bioinspired silver nanostructure by employing betel leaf extract was further confirmed by the characteristic peaks observed in the XRD image (Figure 4). XRD pattern of silver nanoparticles showed numbers of Bragg reflections that may be indexed on the basis of the face-centered cubic structure of silver. A comparison of obtained XRD spectrum with the standard confirmed that the silver particles formed in present experiments were in the form of nanocrystals, as evidenced by the peaks at 2θ values of 38.01, 44.20, 64.37 and 77.34 corresponding to (111), (200), (220), and (311) Bragg reflections, respectively, which may be indexed based on the face-centered cubic structure of silver (JCPDS file nos. 04-0783). X-ray diffraction results clearly show that the silver nanoparticles formed by the reduction of Ag⁺ ions by the betel leaf extract are crystalline in nature. It was found that the average size from XRD data and using the Debye-Scherrer equation was approximately 15nm. The average particle size of silver nanoparticles synthesized by the present green method can be calculated using the Debye-Scherrer equation.^{34,35} The size distribution of the betel leaf extract mediated synthesized AgNPs is depicted in Figure 5. The distribution of the silver nanoparticles observed that the particles obtained are polydisperse mixtures in the size range from 70 to 80nm. The average size of the synthesized silver nanoparticles is around 74nm. The time-dependent fluctuations in the intensity of scattered light that occur are analyzed using an autocorrelator which determines the autocorrelation function of the signal.³⁶

Generally, the sizes and shapes of metal nanoparticles are influenced by a number of factors including pH, precursor concentration, reductant concentration, time of incubation and temperature as well as method of preparation of nanoparticles.³⁷ Umoren et al. observed

red apply fruit extract reduced silver nanoparticles size distribution around 50 to 300 nm and found average size of 150nm. Silver nanoparticles in the size range of approximately 50 to 150nm are synthesized by the supernatant of *Salmonella typhirium* when it is added to silver sulfate.³⁸ SEM analysis shows high-density silver nanoparticles synthesized by betel leaf extract. The particles shape distributions of the silver nanoparticles was observed at different magnifications (Figure 6). It was shown that relatively spherical and uniform silver nanoparticles with high agglomeration were noted. The large silver particles may be due to the aggregation of the smaller ones, due to the SEM measurements. Preetha et al.³⁹ study obtained high density spherical in shape and uniform silver nanoparticles with diameter of 13 to 61 nm synthesized by using cannonball leaf extract.³⁹ The nanoparticles were not in direct contact even within the aggregates, indicating stabilization of the nanoparticles by a capping agent.⁴⁰ In present study, betel leaf extract reduced AgNO₃ to AgNPs shown that relatively spherical and uniform with high agglomeration. Figure 7 shows the EDS photographs of silver nanoparticles, all the peaks of Ag are observed and assigned. Some impurity peaks were detected below 1 keV, corresponds to oxygen, Cl, Na and Ca, which were probably related to the presence of crystalline biomolecules in the extract.⁴¹

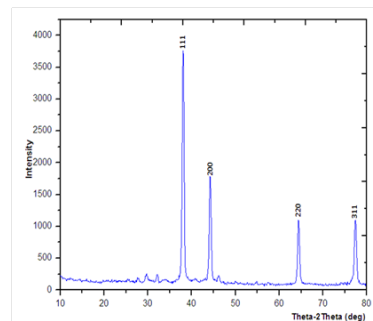


Figure 4 XRD spectrum AgNPs.

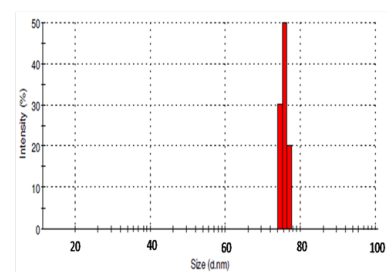


Figure 5 Dynamic Light Scattering measurements of AgNPs.

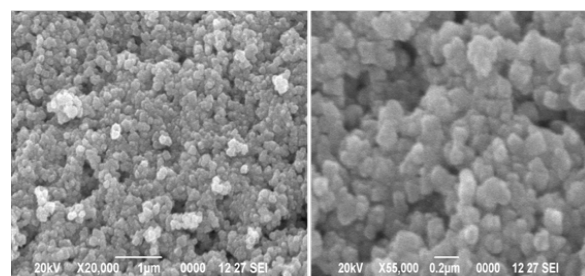


Figure 6 SEM micrograph of silver nanoparticles

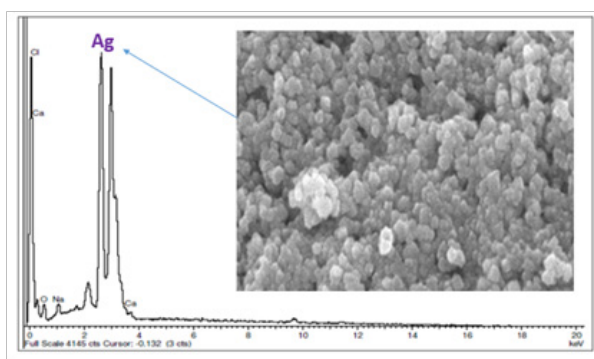


Figure 7 EDS spectrum of AgNPs

Biofilm formation by MTP method

The biofilm is considered as major target for the pharmacological development of drug.⁴² The biofilm index for all the test pathogens were observed in MTP assay (Figure 8). The biofilm index of the test pathogens and OD values were articulated based on the biofilm classification described by Christensen and co-worker.²⁸ The test pathogens considered as strong biofilm producers in MTP assay were *E. coli* (0.294), *S. aureus* (0.292) and *P. aeruginosa* (0.264). Moderate biofilm formation was observed 0.196 OD for *S. epidermidis* and 0.195 OD for *S. epidermidis* respectively (Table 1). The dissimilarity in OD values was due to the amount of crystal violet dye absorbed by the pathogens in the microtitre well.

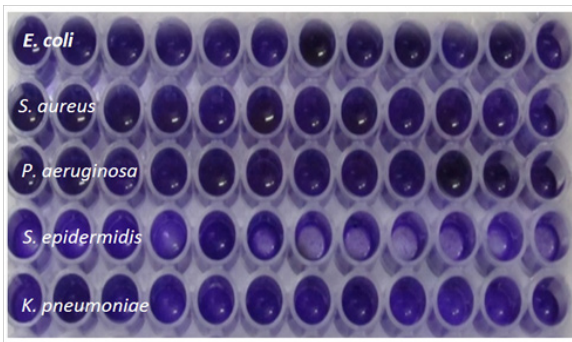


Figure 8 Biofilm forming capability of test bacteria on MTP assay.

Table 1 Screening test bacteria for biofilm formation by MTP method

Test Bacteria	Biofilm formation (OD 570 _{nm})*Biofilm index
<i>E. coli</i>	0.294
<i>S. aureus</i>	0.292
<i>P. aeruginosa</i>	0.264
<i>S. epidermidis</i>	0.195
<i>K. pneumoniae</i>	0.196

Antibacterial activity of AgNPs coated IVC

In this study antibacterial activity of AgNPs coated IVC was evaluated by using standard Zone of Inhibition (ZOI) microbiology assay. Antibacterial activity of after dip-coating with bioinspired synthesis AgNPs catheter materials shows good antibacterial activity against all five test pathogen. Bacterial biofilm formation is considered to be a two-step process^{43,44} bacterial attachment to the foreign

surface and formation of a complex biofilm structure which depends mainly on the synthesis of polysaccharide intercellular adhesion (PIA) encoded by the *ica* ADBS locus which plays a crucial role in mediating the biofilm formation.^{45,46} In the present study, the betel leaf mediated bioinspired synthesized silver nanoparticles coated IVC samples exhibited maximum ZOI was found to be 41mm and 35mm for *K. pneumoniae* and *S. epidermidis* (Figure 9). However, the other three bacteria strains of *E. coli*, *S. aureus* and *P. aeruginosa* showed zone of inhibition of 25, 24 and 22mm respectively (Figure 10). A previous study on the effect of silver nanoparticles on *Pseudomonas putida* biofilms showed at different stages of maturity.⁴⁷ In current study, we found that bioinspired silver nanoparticles dip-coated biomaterial have higher antibacterial action against *S. epidermidis* and *K. pneumoniae*.

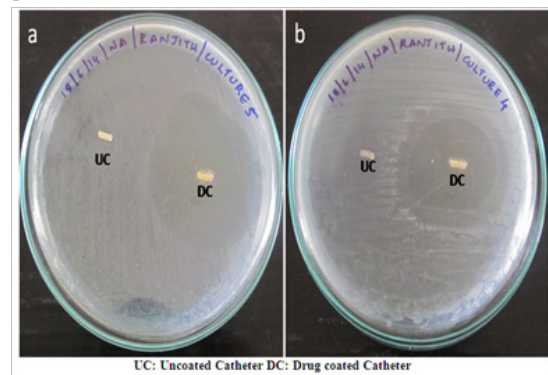


Figure 9 AgNPs coated IVC against (A) *K. pneumoniae*, and (B) *S. epidermidis*

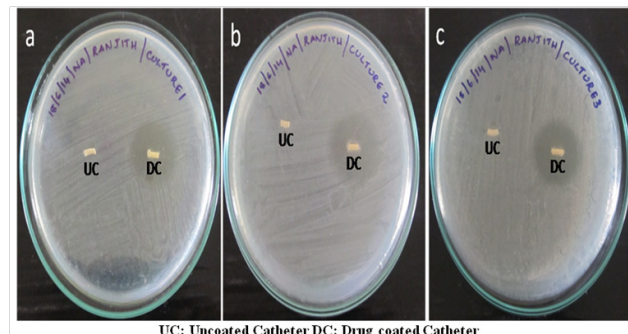


Figure 10 AgNPs coated IVC (A) *E. coli* (B) *S. aureus* and (C) *P. aeruginosa*

Persistence test

Control of biomedical bacterial strains using biogenic AgNPs have been reported extensively.⁴⁸ In SPTT study, silver nanoparticle impregnated with IVC showed a long duration of activities up to Day 7th against *K. pneumoniae* (Figure 11). Bioinspired synthesized silver nanoparticles coated IVC sample exhibited continued inhibition of all tested biofilm producing bacteria except *P. aeruginosa* and *S. aureus*. AgNPs impregnated IVC the zone of inhibition fell steeply and declined to zero on 3rd Day against *S. aureus*. The AgNPs coated biomaterial achieved continued zone of inhibition round 8 mm on 7th Day against *K. pneumoniae* (Figure 12). Previously study by Monzon *et al.* reported that increasing age of *S. epidermidis* biofilms was significantly associated with reduced efficacy of several antimicrobial agents, including cephalothin, clindamycin, erythromycin, vancomycin, and teichoplanin.⁴⁹ In current study, AgNPs impregnated

with IVC showed the zone of inhibition for *E. coli* fell steeply and declined to zero on 5th Day. Franck et al. study reported that the silver nanoparticles impregnation of medical polymers exhibited zone of inhibition was seen for 10 days against clinically isolate *S. epidermidis*.⁵⁰ On another study reported by Zhang and co-worker revealed that silver nanoparticles treated cotton fabric showed 99.01% bacterial reduction of *S. aureus* and bacterial reduced of *E. coli* while the silver content about 88.77%.⁵¹ Similarly, our present study, showed bioinspired AgNPs coated IVC sample exhibit good antibacterial activity against the test pathogens.

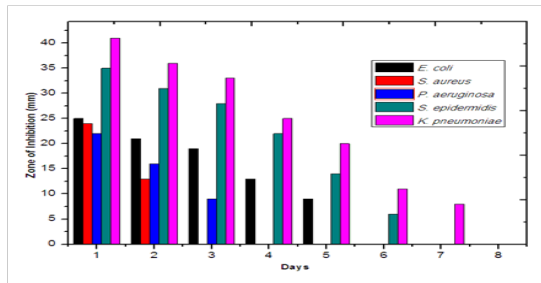


Figure 11 SPTT against biofilm producing organisms.



Figure 12 AgNPs impregnated IVC on 7th Day against *K. pneumoniae*.

Conclusion

Nanotechnology has emerged due to integration of biotechnology with nanotechnology for developing biosynthetic and environmental-friendly technology for synthesis of nanomaterials for biological application. In this present chapter, concentrates on the control of biomedical product biofilm forming bacterial strains using bioinspired synthesized silver nanoparticles around. The betel leaf mediated synthesis silver nanoparticles shown around 70 to 80nm and spherical in shape. Results obtained from the present investigation revealed the betel leaf mediated bioinspired synthesized silver nanoparticles coated IVC biomedical product exhibit potential antibacterial assets against all tested pathogens, particularly the diameter of inhibition zones increased for the test pathogens *S. epidermidis* and *K. pneumoniae*. In addition, persistence test, silver nanoparticle impregnated with IVC exhibited a long duration of activities up to Day 7th against *K. pneumoniae*. In current study suggests biomedical product with specific concentration of AgNPs showed a maximum activity against

biofilm producing organisms. To utilize these potential bioinspired silver nanoparticles may assembled or coated on biomedical product to prevent biofilm formation.

Acknowledgements

Authors are expressing their sincere thanks to Dr NGP Arts and Science College, Coimbatore and CUSAT-STIC, India for their technical support.

Conflict of interest

The authors declare no conflict of interest.

References

1. Branda SS, Vik S, Friedman L, et al. Biofilms: The matrix revisited. *Trends Microbiol.* 2005;13(1):20–26.
2. Schembri MA, Christiansen G, Klemm P. FimH-mediated autoaggregation of *E. Coli*. *Mol Microbiol.* 2001;41(6):1419–1430.
3. Costerton JW, Lewandowski Z, Caldwell DE, et al. Microbial biofilms. *Annu Rev Microbiol.* 1995;49:711–745.
4. Rinaudi LV, Giordano W. An integrated view of biofilm formation in rhizobia. *FEMS Microbiol Lett.* 2010;304(1):1–11.
5. Pablo CB, María de las Mercedes Oliva FG, Sorroche. The Role of Bacterial Biofilms and Surface Components in Plant-Bacterial Associations. *Int J Mol Sci.* 2013;14(8):15838–15859.
6. Rodney MD. Biofilm Formation: A Clinically Relevant Microbiological Process. *Healthcare Epidemiol.* 2001;33(8):1387–1392.
7. Stickler DJ. Bacterial biofilms and the encrustation of urethral catheters. *Biofouling.* 1996;9(4):293–305.
8. Mermel LA, Farr BM, Sherertz RJ, et al. Prevention of intravascular catheter-related infections. *Clin Infect Dis.* 2001;32(5):1249–1272.
9. Mermel LA. Guidelines for the management of intravascular catheter-related infections. *Ann Int Med.* 2000;132(5):391–402.
10. Anassis E, Samonis G, Kontoyiannis D, et al. Role of catheter colonization and infrequent hematogenous seeding in catheter-related infections. *Eur J Clin Microbiol Infect Dis.* 1995;14(2):134–137.
11. Ranjithkumar R, Selvam K, Shanmugavadi M. Green Synthesis of Silver Nanoparticles Using Areca Nut Extract for Enhanced Antibacterial Activity. *J Green Sci Technol.* 2013;1(2):102–206.
12. Theron J, Walker JA, Cloete TE. Nanotechnology and water treatment: applications and emerging opportunities. *Crit Rev Microbiol.* 2008;34(1):43–69.
13. Li Q, Mahendra S, Lyon DY, et al. Antimicrobial nanomaterials for water disinfection and microbial control: potential applications and implications, *Water Res.* 2008;42(18):4591–4602.
14. Jesline PJ, Neetu PM, Narayanan. Antimicrobial activity of zinc and titanium dioxide nanoparticles against biofilm producing methicillin-resistant *Staphylococcus aureus*. *Appl Nanosci.* 2015;5(2):157–162.
15. Julia P, Chevalier Y, Pelletier J, et al. The contribution of zinc ions to the antimicrobial activity of zinc oxide. *Colloid surface A.* 2014;457(5):263–274.
16. Ranjithkumar R, Selvam K, Shanmugavadi M. Antibacterial textile finishing via green synthesized silver nanoparticles. *J Green Sci Technol.* 2013;1(2):111–113.
17. Bindhu MR, Umadevi M. Antibacterial activities of green synthesized gold nanoparticles. *Mat Lett.* 2014;120(1):122–125.

18. Thomas TC, Narvaez RA. The convergence of biotechnology and nanotechnology: Why here, why now? *J Commer Biotechnol.* 2006;12(2):105–110.
19. Inbakandan D, Kumar C, Stanley Abraham L, et al. Silver nanoparticles with anti microfouling effect: A study against marine biofilm forming bacteria. *Colloids and Surface B.* 2013;11(1):636–643.
20. Shanmugavadiu M, Selvam K, Ranjithkumar R. Synthesis of Pomegranate Peel Extract Mediated Silver Nanoparticles and its Antibacterial Activity. *Am J Adv Drug Deliv.* 2014;2(2):174–182.
21. Guggenbichler JP, Boswald M, Lugauer S, et al. A new technology of microdispersed silver in polyurethane induces antimicrobial activity in central venous catheters. *Infection.* 1999;27(1):S16–S23.
22. Hungund BS, Dhulappanavar GR, Ayachit NH. Comparative Evaluation of Antibacterial Activity of Silver Nanoparticles Biosynthesized Using Fruit Juices. *J Nanomed Nanotechnol.* 2015;6:1–6.
23. Haytham MM Ibrahim. Green synthesis and characterization of silver nanoparticles using banana peel extract and their antimicrobial activity against representative microorganisms. *J Radiat Res Appl Sci.* 2015;8(3):265–275.
24. Abdolhossein M, Mina S, Mahere BR, et al. Plant-mediated biosynthesis of silver nanoparticles using *Prosopisfarcta* extract and its antibacterial properties. *Spectrochim Acta Part A.* 2015;141:287–291.
25. Darouiche RO, Raad II, Heard SO, et al. Comparison of two antimicrobial-impregnated central venous catheters. *N Engl J Med.* 1999;340(1):1–8.
26. Wilcox M, Kite P, Dobbins B. Antimicrobial intravascular catheters—which surface to coat? *J Hosp Infect.* 1998;38(4):322–324.
27. Ansari MA, Khan HM, Khan AA, et al. Anti-biofilm efficacy of silver nanoparticles against MRSA and MRSE isolated from wounds in a tertiary care hospital. *Indian J Med Microbiol.* 2015;33(1):101–109.
28. Christensen GD, Simpson WA, Younger JJ, et al. Adherence of coagulase-negative staphylococci to plastic tissue culture plates: a quantitative model for the adherence of staphylococci to medical devices. *J Clin Microbiol.* 1985;22(6):996–1006.
29. Madhumitha G, Selvaraj RM. Devastated Crops: Multifunctional Efficacy for the Production of Nanoparticles. *J Nanomater.* 2013. p. 1–12.
30. Bar HDK, Bhui GP, Sahoo P, et al. Green synthesis of silver nanoparticles using latex of *Jatropha curcas*. *Colloids and Surfaces A.* 2009;339(3):134–139.
31. Khan Z, Bashir O, Hussain JI, et al. Effects of ionic surfactants on the morphology of silver nanoparticles using Paan (Piper betel) leaf petiole extract. *Colloids and Surfaces B.* 2012;98:85–90.
32. Gnanajobitha G, Vanaja M, Paulkumar K, et al. Green Synthesis of Silver Nanoparticles using *Millingtonia hortensis* and Evaluation of their Antimicrobial Efficacy. *Int J Nanomater Biostructures.* 2013;3(1):21–25.
33. Jamil Ahmed M, Murtaza G, Mehmood A, et al. Green synthesis of silver nanoparticles using leaves extract of *Skimmia laureola*: Characterization and antibacterial activity. *Materials Letters.* 2015;153:10–13.
34. Ahmad N, Sharma S, Alam MK, et al. Rapid synthesis of silver nanoparticles using dried medicinal plant of basil. *Colloids Surfaces B.* 2010;81(1):81–86.
35. Nabikhan K, Kandasamy A, Raj NM, et al. Synthesis of antimicrobial silver nanoparticles by callus and leaf extracts from saltmarsh plant, *Sesuvium portulacastrum* L. *Colloids Surfaces B.* 2010;79(2):488–493.
36. Kaszuba M, McKnight D, Connah MT, et al. Measuring sub-nanometre sizes using dynamic light scattering. *J Nanopart Res.* 2008;10(5):823–829.
37. Tomaszecka E, Soliwoda K, Kadziola K, et al. Detection Limits of DLS and UV-Vis Spectroscopy in Characterization of Polydisperse Nanoparticles Colloids. *J Nanomater.* 2013.
38. Umoren SA, Obot IB, Gasem ZM. Green Synthesis and Characterization of Silver Nanoparticles Using Red Apple (*Malus domestica*) Fruit Extract at Room Temperature. *J Mater Environ Sci.* 2014;5:907–914.
39. Preetha D, Prachi K, Chirom A, et al. Synthesis and Characterization of Silver Nanoparticles Using Cannonball Leaves and Their Cytotoxic Activity against MCF-7 Cell Line. *J Nanotechnol.* 2013. p. 1–5.
40. Priya M, Selvan RK, Senthilkumar B, et al. Synthesis and characterization of CdWO₄ nanocrystals. *Ceramics Int.* 2011;37(7):2485–2488.
41. Mie R, Samsudin MW, Din LB, et al. Synthesis of silver nanoparticles with antibacterial activity using the lichen *Parmotrema praesorediosum*. *Int J Nanomedi.* 2014;9:121–127.
42. Karthick Raja Namasivayam S, Christo BB, Karthigai Arasu SM, et al. Anti-Biofilm Effect of Biogenic Silver Nanoparticles Coated Medical Devices against Biofilm of Clinical Isolate of *Staphylococcus aureus*. *Glob J Med Res.* 2013;13(3):25–30.
43. Zheng Y, Li J, Liu X, et al. Antimicrobial and osteogenic effect of Ag-implanted titanium with a nanostructured surface. *Int J Nanomed.* 2012;7:875–884.
44. Milcher GA, Claudi B, Schlegel U, et al. Influence of type of medullary nail on the development of local infection. An experimental study of solid and slotted nails in rabbits. *J Bone Joint Surg Br.* 1994;76(6):955–999.
45. Ariciola CR, Baldassarri L, Montanaro L. Presence of *IcaA* and *IcaD* genes and slime production in a collection of staphylococcal strains from catheter associated infections. *J Clin Microbiol.* 2001;39(6):2151–2156.
46. Rohde H, Frankenberger S, Zahringer U, et al. Structure, function and contribution of polysaccharide intercellular adhesin (PIA) to *staphylococcus epidermidis* biofilm formation and pathogenesis of biomaterial-associated infections. *Eur J Cell Biol.* 2010;89(1):103–111.
47. Thuptimdang P, Limpiyakorn T, McEvoy J, et al. Effect of silver nanoparticles on *Pseudomonas putida* biofilms at different stages of maturity. *J Hazard Mater.* 2015;290:127–133.
48. Kim KJ, Sung WS, Sun BK, et al. Antifungal activity and mode of action silver nano-particles on *Candida albicans*. *Biometals.* 2009;22(2):235–242.
49. Monzon M, Oteiza C, Leiva J, et al. Biofilm susceptibility testing of *Staphylococcus epidermidis* clinical isolates: low performance of vancomycin in relation to other antibiotics. *Diagn Microbiol Infect Dis.* 2002;44(4):319–324.
50. Furno F, Morley KS, Wong B, et al. Silver nanoparticles and polymeric medical devices: a new approach to prevention of infection? *J Antimicrob Chemoth.* 2004;54(6):1019–1024.
51. Zhang F, Wu X, Chen Y, et al. Application of silver nanoparticles to cotton fabric as an antibacterial textile finish. *Fibers and Polymers.* 2009;10(4):496–501.